

STAP AS A SOLUTION FOR HARDWARE IMPERFECTIONS IN MULTI-ANTENNA GNSS RECEIVERS

Emilio Pérez Marcos, Andriy Konovaltsev, Manuel Cuntz, Michael Meurer

*German Aerospace Center (DLR), Institute for Communications and Navigation
Münchner Str. 20, 82234 Wessling, Germany*

Emilio.PerezMarcos@dlr.de, Andriy.Konovaltsev@dlr.de, Manuel.Cuntz@dlr.de, Michael.Meurer@dlr.de

INTRODUCTION AND MOTIVATION

GNSS has become the main technology to provide position and timing services in the world. The increasing dependency of the provided services has raised concerns about the vulnerabilities of the systems. Since GNSS signals travel long distances from the satellites and are emitted with relatively low power, the GNSS signals are very weak when they arrive at the receiver. Thus the signals can be easily blocked by interfering radio transmissions.

The precision provided by current generation GNSS receivers together with the use of sophisticated processing methods leave multipath reception and radio frequency interference as the dominant remaining error sources affecting GNSS performance. These radio frequency interferences are usually of unintentional nature, but they can also be deliberately produced. Unintentional and deliberate interference signals constitute a challenging problem in Safety of Life GNSS applications.

In order to tackle the issue several techniques have been proposed. One of the most powerful technologies arises from the use of antennas formed of several receiving elements. The antenna arrays possess very interesting capabilities, like Null-Steering or Beamforming. Such capabilities, called Spatial Signal Processing algorithms, enable the cancellation or nulling of several interference signals. Loosely speaking the ability of the antenna array to fight interferences depends on the number of elements that form the array. In theory with M elements $M-1$ possible interferences can be attenuated.

Yet there are limitations to the number of antenna elements in the array. Relevant factors are cost and complexity. Antenna design complexity increases with the number of elements and so does the cost. Not only the antenna *per se*, but also the connectors, cabling, amplifiers, filters, number of analogue to digital converters (ADC), etc., increase. In addition to that, given a limited physical space, placing several antenna elements close to each other could lead to undesired interactions that will degrade the performance.

With those ideas in mind, a complementary approach was introduced. By combining Time and Spatial processing it is possible to increase the number of suppressed interference signals without the need of extra elements in the array. This technique based on the use of the temporal and spatial domains is known as Spatial Temporal Adaptive Processing or STAP.

In the last years, with the trend towards software defined radio, the analogue frontend part has taken more and more a backseat in recent research for GNSS receivers. However in the presence of radio frequency interference, an adequate design of the analogue frontend stills plays a crucial role and primarily influences the achievable interference robustness of a GNSS receiver. Any error in the design which causes an information loss can never be entirely recovered by digital processing. In the case of multi-antenna GNSS receivers, the analogue frontend properties are even more crucial for the overall system performance and, therefore, the achievable interference robustness.

In the modern days most array processing techniques are performed in the digital domain. As the name indicates it requires a digitalization process that is carried out by analogue to digital converters (ADCs). There are several types of ADCs based on the particular way that they are implemented. Some literature has been written about how several types of ADCs affect the performance of the GNSS receivers [1][2] but not much has been said about the impact on the previously mentioned array digital processing techniques. Referring to STAP techniques, it is commonly assumed that the ADC provides time uncorrelated samples in an optimum interference free scenario [3][4]. Many array digital processing techniques, not only STAP but also, for example, Beamforming, Direction of Arrival estimation, etc. assume that the so called narrow band signal assumption is fulfilled [5]. Moreover, at least almost identical spectral

characteristics of the different channels are often assumed. That means all channels are assumed to behave exactly the same. However, both assumptions are generally not fulfilled.

The potential of STAP to cope with the effects caused by the narrow assumption and the imperfections of the hardware is investigated. This is performed with the help of extensive numerical simulations under several interferences scenarios.

FRONT END IMPERFECTIONS

For the presented work, a multi-channel superheterodyne frontend was used (see Fig. 1). It comprises three main tasks: filtering, frequency down conversion to an intermediate frequency (IF) and amplification. The Super-heterodyne architecture was preferred against a direct sampling approach. The disadvantage of the direct sampling architecture is that the whole amplification has to be done at a single frequency. This may lead to unwanted resonances. In addition the ADC SNR is highly dependent on the frequency of the input signal. With increasing input frequency the SNR degrades. In phase and in quadrature separation (I/Q-separation) is carried out in the digital domain to avoid I/Q-Imbalances. I/Q imbalances can cause images of interfering signals at mirror frequencies with parapspace. This is especially harmful for spatial interference suppression.

The filtering of the analog signal is carried out in three stages. The first stage is a 20 MHz ceramic band pass filter. A ceramic filter was chosen because of the controllable and almost symmetrical group delay behavior, temperature stability and low insertion loss. The main task for this first filter stage is to suppress out of-band-interference and the unwanted alias of the mixing process of the frequency translation to the first intermediate frequency. The analog mixer is followed by a further filter stage. A inductor capacitor (LC) low pass filter, prevents the local oscillator and RF-break-through signals which unavoidable pass the mixer to enter the IF-amplifiers. The last filtering stage is an antialiasing LC-Filter. This filter type was chosen because of its temperature stability, relatively flat group delay and low insertion loss. Because of their high insertion loss, group delay distortion (triple transit problem) SAW filters are not deployed [6].

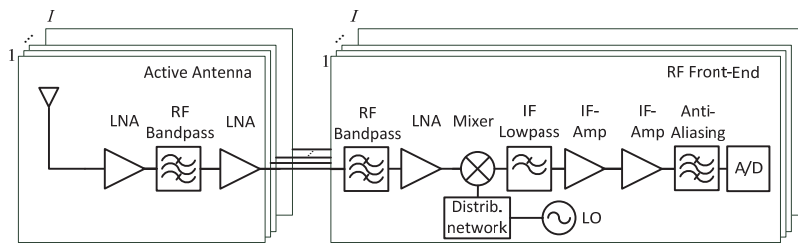


Fig. 1. Block diagram of super heterodyne multi-channel Front End.

The frequency translation of the RF signal to the analog intermediate frequency is done in a single stage. The translation to $f_{IF} = 75$ MHz is carried out by a double balanced mixer.

Due to the ceramic RF filters the unwanted images are suppressed by more than 60 dB. Therefore an image rejection filter at IF-stage is not necessary. The crucial point for a multi-antenna multi-channel Front End is the use of a single PLL-Synthesizer for all channels. The PLL-Phase noise of individual PLL-Synthesizer would strongly degrade pre-correlation adaptive nulling performance. Therefore a dedicated LO-oscillator distribution network was designed. This network distributes the LO signal with equal amplitude and phase to each antenna Front End channel [7].

Signal amplification is a challenging design element for interference robust Front Ends. With the Friis formula the noise figure of the receiving system has to be kept as low as possible. The P1dB compression point of the amplifiers should be as high as possible, but at least high enough to reach the ADC full scale range. In theory, if no RFI is present, the received GNSS signals plus noise should control at least two bits of the ADC [8] to achieve a quantization loss less than 1 dB. Due to sample clock jitter and imperfections in multi-bit ADCs more bits have to be controlled. In practice 5 to 6 bits of a 14-bit ADC have to be controlled by the Front End noise power. This is a trade-off between minimizing quantization losses and maximizing the remaining dynamic range for RFI signals.

In this work while we make an attempt to work with the Front End as close to the reality as possible, we do not want to deal with the mathematic complexity of the models. We will then take the Front Ends as a “black box” that is defined by its measured frequency response, amplitude and phase, and we will use it as a filter to the received signals. In order to obtain the measured frequency response of the Front End a measurement called Vector Mixer has been used [2]. With the cited measurement the so called Scattering parameters are obtained. The S-parameters describe the behavior of

a multi-port network system when incident, reflected and transmitted voltage signals are measured under various stimuli states. Please see Fig. 2 for a measurement setup diagram. For our analysis the S_{21} parameter is of great interest. In general it represents the forward complex transmission coefficient as stated in (1)

$$S_{21} = \frac{\text{Transmitted}}{\text{Incident}} = \frac{b_2}{a_1} \Big|_{a_2=0}. \quad (1)$$

We propose a linear combination of the S-parameter that affects each output. That is, for each output channel we consider the signals incident to this channel and the influence of the signals that are entering the other channels. Depending on the Front End design the contribution of the adjacent channels could be a limiting factor to the performance of the interference mitigation algorithm. Also depending on the different elements in the Front End chain the S_{12} parameter will contain information about non-linear phase or not so flat amplitude response. This also plays a role on the performance of the interference mitigation algorithm.

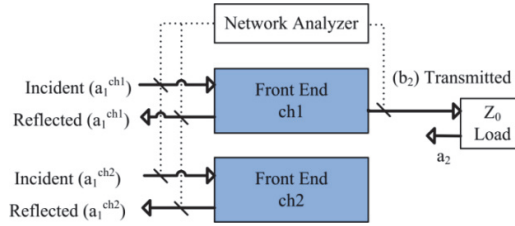


Fig. 2. Front End S-parameter measurement.

INTERFERENCE MITIGATION ALGORITHM

As stated above, the narrowband adaptive beamforming/nulling and STAP will be the chosen algorithms for interference mitigation. First, we introduce a suitable signal model of the array system in order to be able to mathematically define these techniques.

Signal Model

The geometry of the antenna array can be described by a set of vectors \mathbf{p}_m , pointing from the origin of coordinates to the phase center of each of M array elements (see Fig. 3).

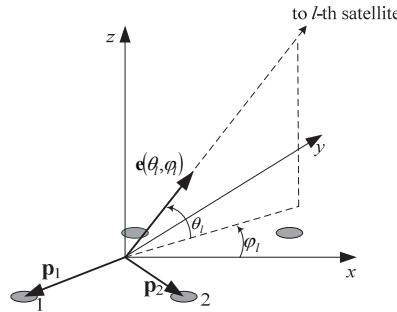


Fig. 3. Antenna array geometry with 4 elements.

The vector containing the array output can be written as:

$$\mathbf{x}(t) = \sum_{l=1}^L \mathbf{s}_l(\theta_l, \varphi_l, t) + \mathbf{n}(t) + \sum_{i=1}^J \mathbf{j}_i(\theta_i, \varphi_i, t), \quad (2)$$

where $\mathbf{s}_l(\theta_l, \varphi_l, t)$ is the component of the received array signal due to the l -th satellite, $\mathbf{n}(t)$ is the received noise and $\mathbf{j}_i(t)$ is the component of the received array signal due to the i -th interference signal. $\mathbf{s}_l(\theta_l, \varphi_l, t)$ can be written as

$$\mathbf{s}_l(\theta_l, \varphi_l, t) = \left[\sqrt{P_l} c_l(t - \tau_l) d_l(t - \tau_l) e^{j(2\pi f_{D,l} t + \phi_l)} \cdot \mathbf{d}(\theta_l, \varphi_l) \right] \cdot \mathbf{H}(\theta_l, \varphi_l, t), \quad (3)$$

where P_l is nominal received power corresponding to the isotropic antenna with unity antenna gain, $c_l(t - \tau_l)$ is the pseudorandom noise (PRN) spreading sequence used by the satellite, $d_l(t - \tau_l)$ is the data modulation, τ_l is the propagation delay of the satellite signal, assuming that group and phase delay are equal, i.e. neglecting the dispersive properties of the ionospheric delay, $f_{D,l}$ is the Doppler frequency offset resulted from the satellite and user motion, $f_{D,l} = -\dot{r} / \lambda$, where \dot{r} denotes the rate of the LOS range, ϕ_l nominal received phase of the carrier, this term also accounts for the carrier phase shift resulted from the propagation delay. $\mathbf{d}(\theta_l, \varphi_l)$ is the array steering vector of the desired signal defined as

$$\mathbf{d}(\theta, \varphi) = \begin{bmatrix} e^{-jk\mathbf{e}(\theta, \varphi)^T \mathbf{p}_1} \\ e^{-jk\mathbf{e}(\theta, \varphi)^T \mathbf{p}_2} \\ \vdots \\ e^{-jk\mathbf{e}(\theta, \varphi)^T \mathbf{p}_M} \end{bmatrix}, \quad (4)$$

where $k = 2\pi/\lambda$ is the wavenumber for a given wavelength λ , $\mathbf{e}(\theta, \varphi)$ is the unit vector pointing towards the satellite direction given by the elevation θ_l and azimuth φ_l . Note that while $\mathbf{s}(\theta_l, \varphi_l, t)$ depends on the elevation and azimuth. For a static or quasi-static scenario it is usually accepted that those change slow compared with t . Equivalently, $\mathbf{j}_i(\theta_l, \varphi_l, t)$ can be written as

$$\mathbf{j}_i(\theta_l, \varphi_l, t) = \left[\sqrt{P_i} z_i(t) \cdot \mathbf{a}(\theta_l, \varphi_l) \right] \cdot \mathbf{H}(\theta_l, \varphi_l, t), \quad (5)$$

where P_i is the nominal received power corresponding to the isotropic antenna with unity antenna gain. $z_i(t)$ is the interference signal. $\mathbf{a}(\theta_l, \varphi_l)$ is the array steering vector of the interference signal and is defined in a similar way as $\mathbf{d}(\theta_l, \varphi_l)$. Of course, the unit vector $\mathbf{e}(\theta, \varphi)$ points in this case towards the interference direction and $k = 2\pi/\lambda$ is given by the interference wavelength.

In both cases the matrix $\mathbf{H}(\theta, \varphi, t)$ accounts for the transfer function of the multiple-input multiple-output block in the signal processing path consisting of the Antenna element and the Front End. As an example, for an antenna array of four elements with four Front End channels we get

$$\mathbf{H}(\theta, \varphi, t) = \begin{bmatrix} h_{ant,1}(\theta, \varphi, t) * h_{FE1,1}(t) & h_{ant,1}(\theta, \varphi, t) * h_{FE1,2}(t) & h_{ant,1}(\theta, \varphi, t) * h_{FE1,3}(t) & h_{ant,1}(\theta, \varphi, t) * h_{FE1,4}(t) \\ h_{ant,2}(\theta, \varphi, t) * h_{FE2,1}(t) & h_{ant,2}(\theta, \varphi, t) * h_{FE2,2}(t) & h_{ant,2}(\theta, \varphi, t) * h_{FE2,3}(t) & h_{ant,2}(\theta, \varphi, t) * h_{FE2,4}(t) \\ h_{ant,3}(\theta, \varphi, t) * h_{FE3,1}(t) & h_{ant,3}(\theta, \varphi, t) * h_{FE3,2}(t) & h_{ant,3}(\theta, \varphi, t) * h_{FE3,3}(t) & h_{ant,3}(\theta, \varphi, t) * h_{FE3,4}(t) \\ h_{ant,4}(\theta, \varphi, t) * h_{FE4,1}(t) & h_{ant,4}(\theta, \varphi, t) * h_{FE4,2}(t) & h_{ant,4}(\theta, \varphi, t) * h_{FE4,3}(t) & h_{ant,4}(\theta, \varphi, t) * h_{FE4,4}(t) \end{bmatrix}, \quad (6)$$

where $h_{ant,m}(\theta, \varphi, t)$ is the response of the m -th antenna array element in the direction given by θ and φ , and $h_{FE,m,n}(t)$ is the response of the Front End connected to the m -th array element to generate the n -th Front End output. Note that $h_{FE,m,n}(t)|_{m \neq n}$ carries information about the crosstalk products due to the Front End channels only. The crosstalk between antenna elements is assumed here to be accounted by the individual transfer functions of the array elements. For this conference paper we will consider $h_{FE,m,n}(t)|_{m \neq n} \triangleq 0$. Note also that (3) and (5) are products of a vector with a matrix hence the result is a vector. The elements of such a vector contain the combination of all the Front End channels affecting its corresponding Front End output.

As this work focuses primarily on the Front End hardware imperfections we make some assumptions in $\mathbf{s}(\theta_l, \varphi_l, t)$ in order to get a simplified model. First, it can be assumed that the antenna array elements are isotropic, i.e. $h_{ant,m}(\theta, \varphi, t) = [1, 1, \dots, 1]^T$. We also neglect the effect of the data modulation, the Doppler offset, and we consider no phase carrier delay. Then Eq. (3) can be written as

$$\mathbf{s}_l(\theta_l, \varphi_l, t) = \left[\sqrt{P_l} c_l(t - \tau_l) \cdot \mathbf{d}(\theta_l, \varphi_l) \right] \cdot \mathbf{H}(t). \quad (7)$$

And Eq. (6) as an example for an antenna of four elements with four Front End channels

$$\mathbf{H}(t) = \begin{bmatrix} h_{FE1,1}(t) & h_{FE1,2}(t) & h_{FE1,3}(t) & h_{FE1,4}(t) \\ h_{FE2,1}(t) & h_{FE2,2}(t) & h_{FE2,3}(t) & h_{FE2,4}(t) \\ h_{FE3,1}(t) & h_{FE3,2}(t) & h_{FE3,3}(t) & h_{FE3,4}(t) \\ h_{FE4,1}(t) & h_{FE4,2}(t) & h_{FE4,3}(t) & h_{FE4,4}(t) \end{bmatrix}. \quad (8)$$

Now $\mathbf{H}(t)$ can be empirically described using the S-parameter method proposed before.

Space Time Adaptive Processing (STAP)

Eq. (2) defines the vector containing the array output at a given time. Still we need to add some formulation to represent the different tap delay components. In order to extend the signal model to be used with STAP, and supposed an antenna array of M elements and a total of K taps, we use the subscript k like $\mathbf{x}_k(t)$. There is no subscript m because it is already implicit in the vector notation. For the first output before any tap we have

$$\mathbf{x}_1(t) = \mathbf{x}(t) = \sum_{l=1}^L \mathbf{s}_l(\theta_l, \varphi_l, t) + \mathbf{n}(t) + \sum_{i=1}^J \mathbf{j}_i(\theta_i, \varphi_i, t). \quad (9)$$

The relation between taps is described as

$$\mathbf{x}_k(t) = \mathbf{x}_1(t - [k-1]T_0), \quad (10)$$

where T_0 accounts for the delay between taps and it is considered to be the same for all antenna elements.

For a given set of antenna elements and taps let $\mathbf{X}_{M,K}(t)$ be the matrix that contains in the columns the vectors of the signals at the k tap of the m -th antenna element

$$\mathbf{X}_{M,K}(t) = [\mathbf{x}_1(t), \mathbf{x}_2(t), \dots, \mathbf{x}_K(t)]. \quad (11)$$

Again note that m subscript is implicit in the \mathbf{x} vector notation. $\mathbf{X}_{M,K}(t)$ is a matrix of M rows and K columns. We can make use of vectorised notation and define

$$\bar{\mathbf{x}}(t) = \text{vec}(\mathbf{X}_{M,K}(t)) = \begin{bmatrix} \mathbf{x}_1(t) \\ \mathbf{x}_2(t) \\ \vdots \\ \mathbf{x}_K(t) \end{bmatrix}. \quad (12)$$

In this work we pursue a Beamformer, so only one signal shall come out from the antenna array (see Fig. 4).

The typical beamforming output is given by

$$\mathbf{y} = \mathbf{w}^H \mathbf{x}. \quad (13)$$

To calculate the optimum weights we start from the Linear Constraint Minimum Variance (LCMV) algorithm. In general terms the criterion for LCMV is

$$\min_{\mathbf{w}} \{ \mathbf{w}^H \mathbf{\Phi}_x \mathbf{w} \} \text{ s.t. } \mathbf{w}^H \mathbf{C} = \mathbf{f}, \quad (14)$$

where $\mathbf{\Phi}_x$ represents the signal covariance matrix, $\mathbf{\Phi}_x = E\{\mathbf{x}\mathbf{x}^H\}$. The weights of the minimization problem are constrained with a matrix \mathbf{C} and a response vector \mathbf{f} . In the case of GNSS signals, before the correlation process, the dominant term in Eq. (9) will be the interference component. In other words, we know that the navigation signal is buried under the noise so the received energy above the noise level will be the interference contribution. We choose to null all signals which exhibit a greater energy than the noise. In order to achieve this we can populate the constraint matrix \mathbf{C} with the desired received direction

$$\min E\{|y(t)|^2\} = \min_{\mathbf{w}} \{ \mathbf{w}^H \mathbf{\Phi}_x \mathbf{w} \} \text{ s.t. } \mathbf{d}^H(\theta, \varphi) \mathbf{w}_i = \mathbf{1}, \quad (15)$$

with

$$\mathbf{w}_i = [w_{1,i}, w_{2,i}, \dots, w_{M,i}]^T \quad (16)$$

being the weighting coefficients, that belong to the i tap. It is a usual practice to choose $i = (K+1)/2$ as the central tap of an odd amount of taps. With the mentioned constraint we guarantee a constant gain at the desired direction. No mitigation shall be applied to signals coming from (θ_i, φ_i) .

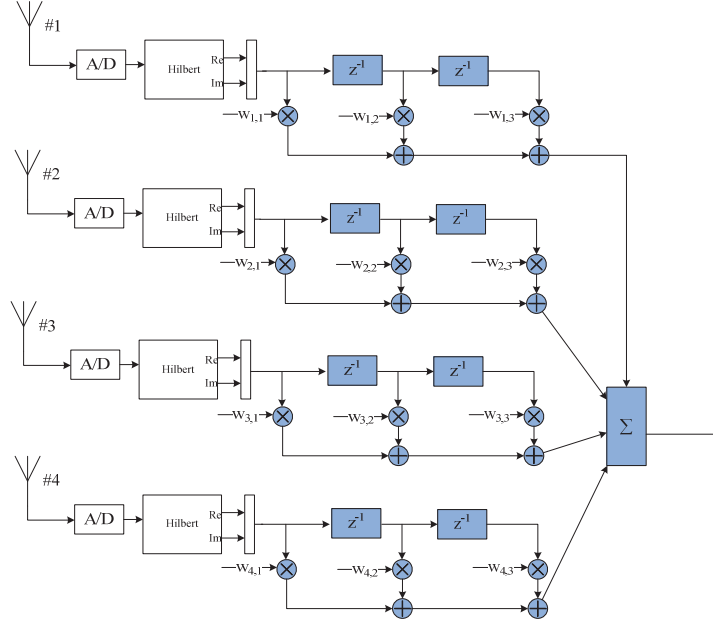


Fig. 4. STAP Beamforming architecture with 4 antenna elements and 3 taps.

The weights are then calculated as

$$\mathbf{w} = \frac{\mathbf{\Phi}_x^{-1} \mathbf{C}}{\mathbf{C}^H \mathbf{\Phi}_x^{-1} \mathbf{C}} \mathbf{f} = \frac{\mathbf{\Phi}_x^{-1} \mathbf{d}(\theta, \varphi)}{\mathbf{d}^H(\theta, \varphi) \mathbf{\Phi}_x^{-1} \mathbf{d}(\theta, \varphi)}. \quad (17)$$

That it is the known Minimum Variance Distortionless Response (MVDR) or Capon Beamformer.

That assumes some kind of knowledge about the desired steering vector (almanac, estimation, etc.). If we do not know where the desired signals are coming from we can just use

$$\mathbf{d}^H(\theta, \varphi) = \mathbf{e} = [0, \dots, 0, 1, 0, \dots, 0]^T. \quad (18)$$

The directional constraint is not known, so the optimization goal is to get an omnidirectional pattern, attenuating only the directions where received energy is bigger than noise. This mitigation process is also called “nulling” because it does not really perform any proper beamforming. That is also why Eq. (15) is also described as $\min E\{|y(t)|^2\}$. It is

worth to mention that $\mathbf{\Phi}_x = E\{\mathbf{x}\mathbf{x}^H\}$ is unknown and therefore has to be estimated. Second-order statistics have been deeply studied and, for the covariance case, a good estimator in terms of maximum likelihood is given by

$$\mathbf{R}_x = \hat{\mathbf{\Phi}}_x = \frac{1}{N} \sum_{i=1}^N \mathbf{x}\mathbf{x}^H, \quad (19)$$

where \mathbf{R}_x is the estimated covariance matrix taking N samples of the array output. The estimated covariance matrix can be updated block wise or use some kind of time average. The block method processes a number N of samples, estimates the covariance and then starts with the next block of N samples. The size of N accounts for the quality of the estimation, no ill conditioned matrix is desired. But the size of N samples accounts also for the dynamics of the system, defining how fast a new estimation will be produced. That plays a role for fast moving scenarios, intermittent interferences and so on.

For the time average we use an exponential moving average defined as

$$\mathbf{R}_x[n+1] = \gamma \mathbf{R}_x[n] + (1-\gamma) \mathbf{x}[n] \mathbf{x}^H[n], \quad (20)$$

where $\gamma \in \mathbb{R} : \{0,1\}$ is the memory factor accounting for how much of the old estimation shall be used in the new one.

RESULTS AND CONCLUSIONS

The simulations are used to support the statements presented in the introduction. We used an interference $z_i(t)$ modeled as strong wideband band limited noise signal. The interference characteristics are: interference to noise ratio (INR) of 63 dB; bandwidth of 20 MHz - that is directly centered at the receiver frequency of interest -; and imping elevation of 65 degrees.

We would like to illustrate the effects of introducing our Front End between the received signals and our interference mitigation algorithm. The Front End is modeled as a filter with a response obtained from the S-parameters of an actual real measured Front End (see Fig. 5). In a channel to channel analysis not only amplitude variations are observed, but also phase differences. In addition, the phase of each channel is not completely linear. That is better understood by looking at Fig. 5 (c), where the group delays of each channel is plotted in reference to the first one.

Fig. 6 compiles the STAP responses where different number of taps was used. From the results we conclude that the Front End shifts the spatial position of the null. Adding more taps to the system seems to improve the accuracy of the position, yet from certain number of taps there is no clear improvement. Regarding the quality of the null position, it makes sense to point out a couple of things. First, for this particular test, STAP is attenuating interferences based only on energy received, i.e. no known desired direction is available (no MVDR) and, what is more important, no Front End specific modification has been made to the STAP algorithm, the constraint matrix \mathbf{C} is not changed neither is the response vector \mathbf{f} . The analysis of such potential modifications will be cover in future work.

While the quality of the spatial null positioning suffered due to the Front End imperfections, the spectral attenuation and the available bandwidth sensitivity are kept (see Fig. 7 and Fig. 8) thanks to the STAP technique. The narrowband beamformer, with its one tap, provides an almost band constant and not very strong attenuation. Whilst with the STAP beamformer the null are increasingly deeper and a better definition for the exclusion band is available. The amount of taps required to achieve positive results is higher than without the Front End inclusion.

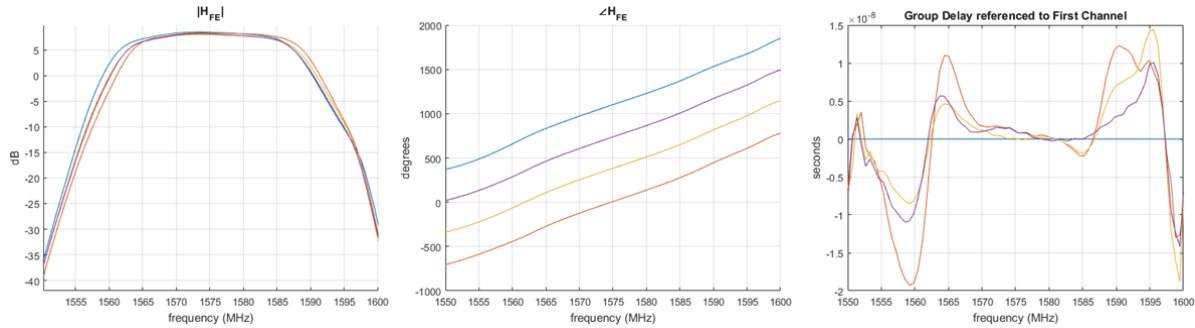


Fig. 5. Front Model based on S_{21} parameter. (a) Amplitude, (b) Phase and (c) Group delay referenced to first channel.

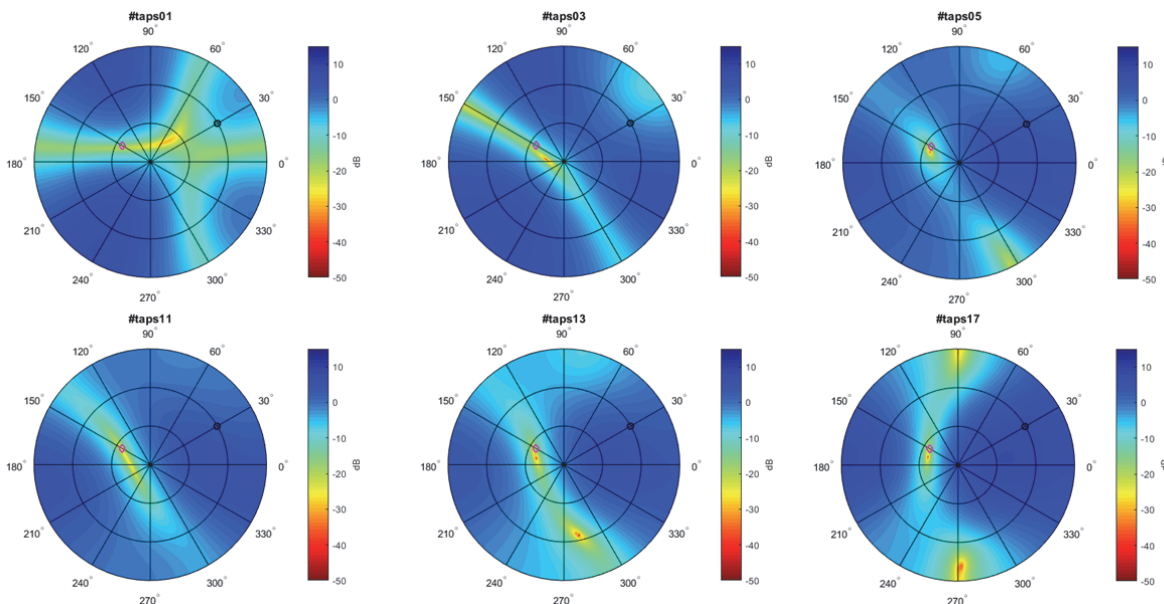


Fig. 6. STAP spatial response. Interference indicated by the red diamond, SV by a black dot.

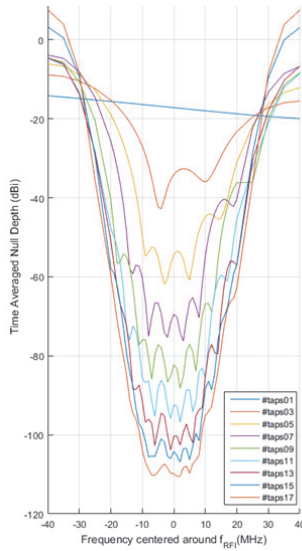
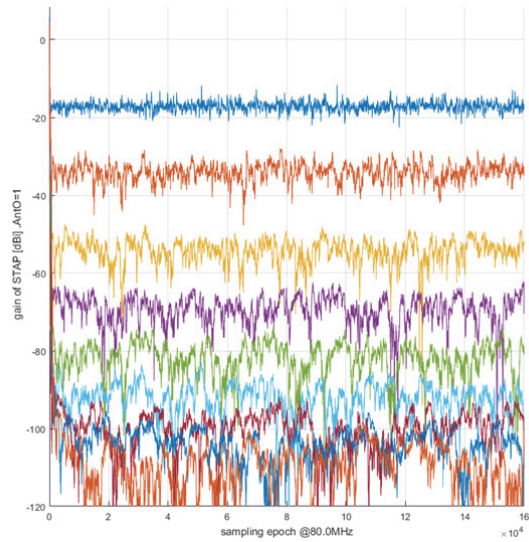


Fig. 7 (a) Null depth in frequency



(b) Null depth: time evolution

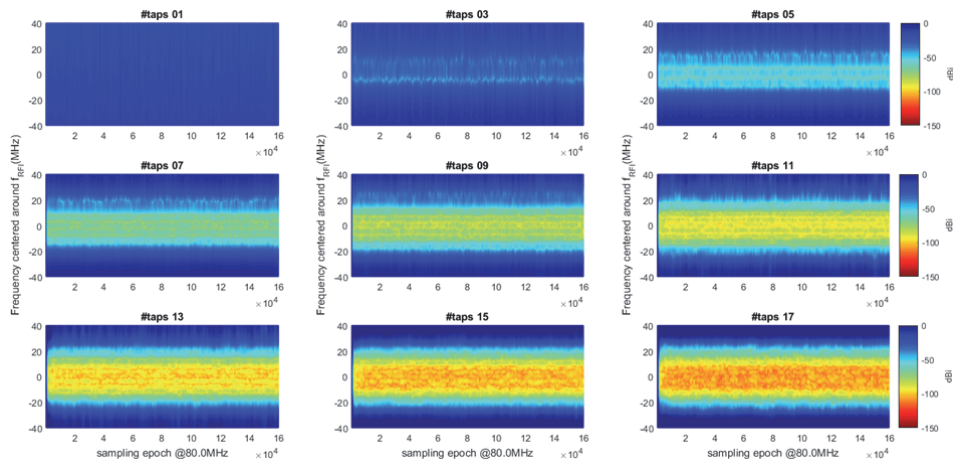


Fig. 8 STAP Spectrogram centered at the interference frequency.

[1] J. J. Spilker and F. D. Natali, "Interference Effects and Mitigation Techniques," in *Global Positioning System: Theory & Applications*, B. W. Parkinson and J. J. Spilker, Eds. American Institute of Aeronautics and Astronautics, Inc., 1996, p. 793.

[2] P. W. Ward, "What's going on? RFI Situational Awareness in GNSS Receivers", *Insid. GNSS*, no. September/October, pp. 34–42, 2007.

[3] R. Fante and J. Vaccaro, "Wideband cancellation of interference in a GPS receive array", *Aerosp. Electron. Syst. IEEE ...*, vol. 36, no. 2, 2000.

[4] H. L. Van Trees, *Optimum Array Processing (Detection, Estimation, and Modulation Theory, Part IV)*. Wiley-Interscience, 2002.

[5] M. Zatman, "How narrow is narrowband?", *IEE Proc. - Radar, Sonar Navig.*, vol. 145, no. 2, p. 85, 1998.

[6] D. Adams. *Effects of SAW Group Delay Ripple on GPS and GLONASS Signals*, [Online]. Available: <http://www.novatel.ca/Documents/Papers/gpsandglonasssignals.pdf>

[7] M. Cuntz et al, "Lessons Learnt: The Development of a Robust Multi-Antenna GNSS Receiver," In 23rd Int. Tech. Meeting of the Satellite Division of The Institute of Navigation (ION GNSS 2010), Portland, OR, 2010, pp. 2852-2859.

[8] F. Bastide, "Analysis of the Feasibility and Interests of Galileo E5a/E5b and GPS L5 Signals for Use with Civil Aviation," Dissertation, Institut National Polytechnique de Toulouse, Toulouse, France, 2004.